공학석사학위논문

Bayesian Network for Structures Subjected to Sequence of Main and Aftershocks

구조 시스템의 본진−여진 시퀀스 베이지안 네트워크 구축

2019 년 8 월

서울대학교 대학원

건설환경공학부

문 창 욱

Abstract

Civil infrastructure systems demand a careful preparation against catastrophic natural hazards such as earthquake. In general, strong earthquakes are accompanied by aftershocks, and thus the seismic risk assessment for upcoming aftershocks is essential for decision making regarding disaster risk management, evacuation from damaged building. The risk assessment should take into account many factors, which are related to the characteristics of main and aftershocks, and state of the structure under the sequence.

For such complex events, the Bayesian network (BN) can be a powerful tool to model probabilistic relationship between multiple random variables describing the earthquake event, and perform probabilistic inference given observation or assumption of states. A BN represents the relationship between random variables by a directed acyclic graph, for which the information regarding conditional distribution of each random variable given its parent nodes.

In this study, artificial ground motions are used to reflect the stochastic properties of main and aftershocks ground motions in dynamic analysis with structural model which is capable of describing structural damage. The features of the processes are represented in the BN that describes their causal relationships. In this modeling, general BN methods would need complete description of random variables, e.g. structural response to infeasible shape of ground motions, and thus yield a memory issue in implementation. To solve this problem, Matrix-based Bayesian network (MBN) is utilized for efficient modeling of BNs.

Using the proposed BN, the Fragility, i.e. the conditional failure probability of

a structural system given an intensity of ground motions, is evaluated to assess the multi-hazard risk of main and aftershocks. This conditional probability can be directly evaluated by the probabilistic inference of the BN model. Furthermore, the fragility of structures is evaluated with related to the intensity measure of main shock as well as that of aftershocks to show the effect of structural damage under the main shock on the fragility of aftershocks. The fragility assessment using BN model is demonstrated by numerical investigations.

Keywords: Main shock, Aftershock, Bayesian network, Matrix-based Bayesian network, Probabilistic inference, Fragility

Student Number: 2017-28720

Table of Contents

List of Figures

List of Tables

Chapter 1. Introduction

In 2016, Gyeongju earthquake with magnitude 5.8 occurred in South Korea with following aftershocks as shown in Figure 1.1. The aftershocks continued to occur for several months, which made people in the area anxious about additional aftershocks. This anxiety worsened by lack of experience to cope with the occurrence of earthquakes in South Korea. In order to make urban communities reliable against such sequential earthquake events, it is necessary to quantify the risk of not only the strong main shock but also the following aftershocks under the aftermath of the main shock. The seismic risk analysis requires probabilistic modeling because earthquake events contain significant uncertainties. Based on the probabilistic modeling, the fragility, i.e. the conditional failure probability given the value of seismic intensity measure (IM), can be estimated to quantify the risk of aftershocks as well as main shock.

To evaluate the fragility of structural systems, probabilistic relationship between IM and structural response, or Engineering Demand Parameters (EDP) is derived based on the results of dynamic analysis. Incremental dynamic analysis (Vamvatsikos and Cornell 2002) is one of the widely used methods, in which ground motions are scaled until the structural system shows the failure. In contrast to the IDA, Jalayer (2003) presented the so-called cloud analysis which estimates the fragility using the linear regression for logarithm of EDP and IM. In the process, the behavior within failure range is regressed based on an assumed mathematical form, so the scaling of ground motions is not needed. Later, Jalayer *et al*. (2015) further developed the cloud analysis with Bayesian framework to incorporate the

uncertainty in ground motion record or structural modeling. Miano *et al*. (2018) exploited the cloud analysis to implement IDA with minimal scaling of ground motions. Multiple stripe approach (MSA) also used ground motions scaled with intervals to derive the fragility based on closed form of probability distribution (Baker 2015). However, the estimated fragility will be different depending on not only the assumed relationship between IM and EDP but also the ground motions used for dynamic analysis. The approaches of using scaled ground motions can yield different results according to the other properties of ground motion such as frequency contents or duration of motion (Iervolino *et al*. 2006). In addition, the closed form representing the relationship may not be adequate if a structural system shows severe nonlinearity, and consequently requires another IM which is well fitted to the closed form with EDP.

In order to reflect possible characteristic of real ground motions, artificial ground motions can be used. Artificial ground motions can be generated by filtering the white noise process which has a uniform power spectral density (PSD). The frequency response of a single degree of freedom (SODF) oscillator under the white noise is used (Kanai-Tajimi model) to estimate the PSD of ground acceleration. The artificial time histories are then simulated based on sinusoidal basis functions (Shinozuka and Deodatis 1991). The acceleration response of an SODF oscillator under the white noise can be exploited directly to simulate ground motions in which the impulse response function (IRF) is used as a filter (Rezaeian and Der Kiureghian 2008). Although the Kanai-Tajimi and IRF filters are feasible to simulate artificial ground motions having the same statistical properties with real records, the stochastic model developed by Rezaeian and Der Kiureghian (2008) is used in this

study because the parameters used in the model can be utilized in probabilistic model with their correlation coefficients. Furthermore, the parameters can be regressed based on the seismological data of main and aftershock (Rezaeian and Der Kiureghian 2008, Hu *et al*. 2018), which helps to develop a probabilistic model of main and aftershocks.

In the literatures, fragility for main and aftershocks have been assessed with elaborate structural model and prescribed damage state. Ryu *et al*. (2011) developed fragility for structures damaged by main shock by performing IDA on a nonlinear SDOF model with a multi-linear hysteresis in which Spectral acceleration (Sa) and the peak displacement are used as IM and EDP respectively. The damage state after main shock is described in terms of the peak response under main shock. Shin *et al*. (2014) compared the fragility of damaged piloti-type RC building with the structure retrofitted with buckling-restrained braces. For the PGA and the maximum inter-story drift ratio (IDR), fragility is estimated with lognormal distribution assumption. Wen *et al*. (2017) compared the EDPs, e.g. peak roof displacement, IDR, residual roof displacement, hysteretic energy, and used the modified Park-Ang damage index, which incorporates dissipated hysteresis energy as well as displacement-based measure, to show the vulnerability under main and aftershock using fragility of a frame structure with Sa as the IM. Though theses fragilities were well evaluated for the given condition, there is no consistent probabilistic model to incorporate the factors related to the main and aftershocks.

This study aims to develop a comprehensive probabilistic model using the Bayesian network (BN), which is needed to estimate the consistent fragility of structural system and update the fragility under the sequential earthquake event. The

sequence of main and aftershocks is a complex natural event, but its components should have an apparent causal relationship which BN model can intuitively represent. Especially, Matrix-based Bayesian Network (MBN) enable the modeling of BN with essential data, which consequently facilitates efficient probabilistic inference using the BN model. This study shows that probabilistic inference of the BN model, which is based on MBN, is utilized to estimate aftershock fragility considering structural damage under main shock with numerical investigations.

The rest of the thesis is organized as follows. Chapter 2 provides the concept of fragility and a brief introduction of the BN model and inference. Chapter 3 presents BN-based probabilistic model for the sequence of main and aftershocks. The structural response under the sequential earthquakes is incorporated into the BN model in Chapter 4, in which the damage caused by main shock is described probabilistically. Based on the BN framework, the estimation of aftershock fragility is shown with the examples of Single Degree of Freedom (SDF) and Multi Degree of Freedom (MDOF) systems in Chapter 5. Finally, Chapter 6 summarizes the study with concluding remarks.

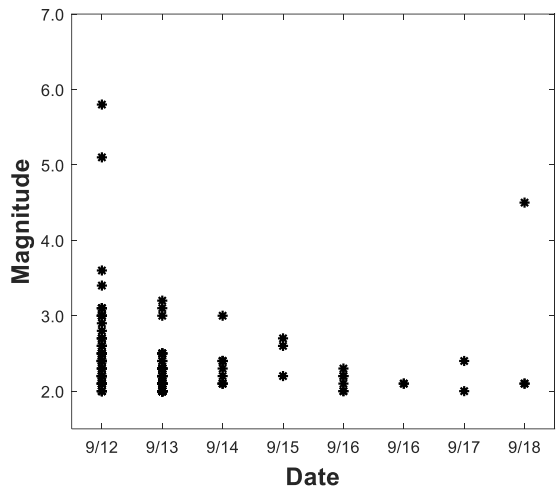

Figure 1.1 Magnitude of main and aftershocks in 2016 Gyeongju Earthquake
(Data Source: Korea Meteorological Administration)

Chapter 2. Theoretical Background

2.1. Concept of fragility

The framework of Performance Based Earthquake Engineering (PBEE) presents a way of probabilistic evaluation for earthquake performance. The main objective of the framework is to evaluate structures considering uncertainties in earthquake events and structural behavior, and provide a measure of performance to stakeholders so that they can make risk-informed decisions (Moehle and Delerlein 2004). One step in the PBEE framework is to estimate the fragility of structural systems, which is the conditional failure probability of structures given the intensity of ground motions (IM). The response of structures under the ground motion is called Engineering Demand Parameters (EDP), and the failure of structures is usually defined as the event that EDP exceeds the prescribed capacity, i.e.

$$\text{Fragility} = \text{P}(EDP \geq EDP_c | IM) \tag{2.1}$$

where EDP_c is the prescribed capacity of the EDP. In order to estimate the fragility, dynamic analysis with a set of ground motions is often performed. Base on the result of the analysis, probabilistic relationship between EDP and IM is constructed. The exceedance probability is then calculated using the relationship. Accordingly, the fragility of structures depends on not only the probabilistic relationship but also the set of ground motion used for dynamic analysis. This study use Bayesian Network to construct a probabilistic model which can incorporate the property of ground motions sufficiently as well as describe the probabilistic relationship accurately.

2.2. Introduction to Bayesian network

Bayesian Network (BN) is one of the widely used probabilistic models (Koller and Friedman, 2009), which is useful in construction of joint distribution for many random variables (r.v.'s). In the BN model, dependency of r.v.'s are represented as a directed acyclic graph in which nodes arcs represent r.v.'s and their statistical dependencies respectively. Figure 2.1 shows a simple example of BN model. Since the structure of overall r.v.'s is expressed graphically, causal relationship between r.v.'s can be modeled and presented intuitively. The dependent r.v.'s are called child nodes while affecting r.v's are termed parent nodes. For example, in Figure 2.1, the child nodes of X_1 are X_2 and X_3, and the parent node of X_2 (or X_3) is X_1. To define the BN model, the conditional distribution is required at each nodes. If there is no parent node (X_1), the conditional distribution is to be marginal distribution (conditional distribution given null event is to be marginal distribution). The joint distribution of r.v.'s are expressed as the multiplication of each conditional distribution at nodes. The example BN in Figure 2.1 describes the joint distribution as follows:

$$P(X_1, X_2, X_3) = P(X_1)P(X_2|X_1)P(X_3|X_1) \tag{2.2}$$

where $P(X_2|X_1)$ and $P(X_3|X_1)$ are conditional distribution of X_2 given X_1, and that of X_3 given X_1, respectively.

The representation of joint distributions by BN is an efficient way to construct probabilistic model for multiple r.v.'s. The marginal distribution of a r.v. can be derived from the BN by efficient algorithm developed for marginalization of the joint

distribution. According to the Bay's rule, the posterior distribution of a r.v. Y when other r.v. X is observed to have a value e is calculated as follows:

$$\mathrm{P}(Y|X=e)=\frac{\mathrm{P}(X=e|Y)}{\mathrm{P}(X=e)}\,\mathrm{P}(Y) \tag{2.3}$$

Since the joint distribution is known, the posterior distribution of r.v.'s in BN is calculated by Eq. 2.3. For example, the posterior distribution of X_3 given $X_2=e$ is calculated as follows:

$$\begin{aligned}\mathrm{P}(X_3|X_2=e)&=\frac{\mathrm{P}(X_2=e|X_3)}{\mathrm{P}(X_2=e)}\mathrm{P}(X_3)\\&=\frac{P(X_2=e,X_3)}{P(X_2=e)}=\frac{\sum_{X_1}P(X_1)P(X_2=e|X_1)P(X_3|X_1)}{\sum_{X_1}\sum_{X_3}P(X_1)P(X_2=e|X_1)P(X_3|X_1)}\\&=\frac{\sum_{X_1}P(X_1)P(X_2=e|X_1)P(X_3|X_1)}{\sum_{X_1}P(X_1)P(X_2=e|X_1)}\end{aligned} \tag{2.3}$$

In this way, the distribution of r.v.'s in BN model can be updated when new information is observed or assumed. The probabilistic inference is a process to obtain conditional distribution given observation, which can be thus applied to the calculation of fragility.

The probabilistic inference is based on the elimination of nodes which is not of interest, e.g. X_1 in Eq. 2.3. This elimination is performed by summing the joint distribution of r.v.'s over the nodes to be eliminated. For example, the r.v. X_2 of example BN in Figure 2.1 can be eliminated by summing the joint distribution in Eq. 2.2 as follows:

$$
\begin{aligned}
P(X_1, X_3) &= \sum\nolimits_{X_2} P(X_1, X_2, X_3) \\
&= \sum\nolimits_{X_2} P(X_1) P(X_2|X_1) P(X_3|X_1) \\
&= P(X_1) P(X_3|X_1) \sum\nolimits_{X_2} P(X_2|X_1) = P(X_1) P(X_3|X_1)
\end{aligned}
\tag{2.4}
$$

The summation operator is actually performed for the terms which contain the nodes to be eliminated. For a BN with multiple variables, this process is repeatedly performed until the variables of interest only remain. This process is so-called *sum-product variable elimination*, which is a basic algorithm for probabilistic inference. For a complex BN model, the algorithm may need a lot of time to converge, so advanced algorithms is required to efficiently eliminate variables.

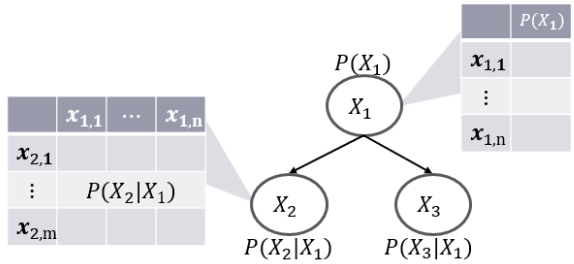

Figure 2.1 Simple example of Bayesian network

Chapter 3. BN-based Seismic Sequence Model

3.1. Stochastic model for artificial ground motions

Real ground motions show characteristics such as nonstationarity of intensity and frequency contents. The response of a structural system is sensitive to such ground motion properties that can be different even if ground motions have the same IM, e.g. PGA, Sa. Consequently, the fragility of a structural system depends on the set of ground motions selected for structural dynamic analysis. For consistent evaluation of the fragility of structural system, it is thus necessary to select adequate ground motions. In this study, simulated ground motions are used to reflect their properties effectively in BN.

The characteristics of real ground motions are specified in a way that their variation in time and spectral domain are considered. In the time domain, the intensity of ground motions generally increases from the starting point until reaching a stable value, and decreases to zero after a strong motion duration. In the spectral domain, the frequency contents of ground motions usually shift from high to low frequency range because of the gap between the arrival time of P waves, S waves and surface wave (Rezaeian and Der Kiureghian 2008).

Rezaeian and Der Kiureghian (2008) developed a stochastic model to simulate synthetic ground motions with nonstationary properties described above. The stochastic modeling starts with the white noise process, which has a uniform contribution from the frequency domain. There are two transformation (or filtering) to change the white noise process to achieve consistency with real ground motions.

The frequency contents and intensity are changed at each transformation separately. The mathematical expressions of the two transformations are as follows:

$$x(t) = q(t, \boldsymbol{\alpha}) \left\{ \frac{1}{\sigma_h(t)} \int_{-\infty}^{t} h[t - \tau, \boldsymbol{\lambda}(\tau)] \omega(\tau) \mathrm{d}\tau \right\} \tag{3.1}$$

where $x(t)$ is the process after the two transformation, $\omega(\tau)$ is the white noise process, $h[t - \tau, \boldsymbol{\lambda}(\tau)]$ is the impulse response function (IRF) with time-varying model parameters $\boldsymbol{\lambda}(\tau)$, $\sigma_h(t)$ is the standard deviation of the integral process, and $q(t, \boldsymbol{\alpha})$ is time-modulating function.

The randomly generated white noise process $\omega(\tau)$ is transformed using the following IRF, which is defined as the acceleration response of an SDOF system under unit impulse load:

$$\begin{aligned} h[t - \tau, \boldsymbol{\lambda}(\tau)] &= \frac{\omega_f(\tau)}{\sqrt{1 - \zeta_f^2}} \exp\left[-\zeta \omega_f(\tau)(t - \tau)\right] \sin\left[\omega_f(\tau) \sqrt{1 - \zeta_f^2}(t - \tau)\right], \tau \le t \\ &= 0 \quad \text{otherwise} \end{aligned} \tag{3.2}$$

The IRF has model parameters of $\omega_f(\tau)$ and ζ_f which denote the natural frequency and damping ratio of the SDOF system, respectively. The natural frequency $\omega(\tau)$ affects the dominant frequency of simulated ground motions, in which the natural frequency is defined as a linear function as follows

$$\omega_f(\tau) = \omega_{mid} + \omega'(\tau - t_{mid}) \tag{3.3}$$

where ω_{mid} is the natural frequency at time t_{mid} and ω' is the variation of the natural frequency per unit time. t_{mid} denotes the time at the middle of the strong-shaking phase which is a parameter for the time modulating function. By using the

linearly varying natural frequency of the SDOF system, the simulated ground motions also can have time-varying dominant frequency as real ground motions. The damping ratio affects the bandwidth of simulated ground motions, so three model parameters ($\omega_{mid},\ \omega',\ \zeta_f$) are necessary to define the IRF function and control the frequency contents of generated ground motions. After that, transformed process (integral process) is normalized by its standard deviation

$$\sigma_h = \left[\int_{-\infty}^{t} h^2[t-\tau, \boldsymbol{\lambda}(\tau)]\mathrm{d}\tau\right]^{1/2} \tag{3.4}$$

The normalized process, which is expressed in the bracket $\{\cdot\}$ of Eq. 3.1, has unit variance, so the intensity and frequency of generated ground motion can be separately controlled by the IRF and the time-modulating function.

The time modulating function is

$$q(t, \boldsymbol{\alpha}) = \alpha_1 t^{\alpha_2 - 1}\exp(-\alpha_3 t) \tag{3.5}$$

where $\alpha_1,\ \alpha_2$, and α_3 are the model parameter of the time modulating function. At this time, the parameters of time-modulating function ($\alpha_1,\ \alpha_2,\ \alpha_3$) have no physical meanings related to ground motion, so they are transformed to three physical terms: $\bar{I}_{\mathrm{a}}$, D_{5-95}, and t_{mid}. $\bar{I}_{\mathrm{a}}$ is the expected Arias intensity. D_{5-95} denotes the effective duration of the motion, which is defined as the time interval between 5 and 95% levels of the expected Arias intensity. t_{mid}, which is already described in Eq. 3.3, is as the time point when 45% level of the expected Arias intensity. The transformation from ($\alpha_1,\ \alpha_2,\ \alpha_3$) to ($\bar{I}_{\mathrm{a}},\ D_{5-95},\ t_{mid}$) is based on the definition of the expected Arias intensity, which is

$$\bar{I}_{\mathrm{a}} = E\left[\frac{\pi}{2g}\int_0^{t_n} x^2(t)dt\right] = \frac{\pi}{2g}\int_0^{t_n} q^2(t,\boldsymbol{\alpha})dt \tag{3.6}$$

where g is the gravitational acceleration and t_n is the duration of ground acceleration. The second equality in Eq. 3.6 is acquired by the following relationship

$$E[x^2(t)] = q^2(t,\boldsymbol{\alpha})E\left[\left\{\frac{1}{\sigma_h(t)}\int_{-\infty}^{t} h[t-\tau,\boldsymbol{\lambda}(\tau)]\omega(\tau)\mathrm{d}\tau\right\}^2\right] = q^2(t,\boldsymbol{\alpha}) \tag{3.7}$$

where the expectation in second term represents the variance of the normalized process.

A random process $x(t)$ generated by Eq. 3.1 has a tendency to overestimate the response of long period structural system compared to the corresponding real ground motions. To alleviate the phenomenon, $x(t)$ is filtered using a critically damped oscillator (high-pass filter) which has the natural frequency of ω_c. The post-process has little influence on the frequency contents except low frequency range (long period contents) and helps assure zero residual of velocity and displacement of generated ground motions. The high-pass filtered process $\ddot{z}(t)$ can be obtained by solving the following equation of motion:

$$\ddot{z}(t) + 2\omega_{\mathrm{c}}(t)\dot{z}(t) + \omega_c^2(t)z(t) = x(t) \tag{3.8}$$

3.2. BN modeling of single ground motion

Section 3.1 introduced a stochastic model that is described by the six model parameters $\bar{I}_{\mathrm{a}}$, D_{5-95}, t_{mid}, ω_{mid}, ω', ζ_f. The model parameters determine the statistical properties of generated ground motions in terms of intensity and frequency contents as demonstrated in Figure 3.1 and 3.2. Accordingly, the model parameters can be considered as the *cause* of generated ground motions, while the IM of the ground motions can be an *effect* of the cause. This causal relationship can be represented in a BN model as Figure 3.3, and the conditional distribution of IM given model parameters can be estimated from the simulated of ground motions. Furthermore, multiple IMs could be used for the same set of ground motions, which would enable us to assess fragility given multiple IMs.

The properties of ground motions would vary according to the location of the structural system. For example, countries near an earthquake zone are more susceptible to strong earthquakes compared to those far from a zone. Rezaeian and Der Kiureghian (2010) developed a regression model to relate model parameters with site and source effects of earthquake events using strong motion records mainly from the PEER NGA database. In the regression model, fault type (F), magnitude (M), source-to-site distance (R_{rup}), and site shear-wave velocity (V_{s30}) are used to represent the features of earthquake scenario. The relationship between earthquake scenario and the model parameters can be modeled as a BN model as illustrated in Figure 3.4, and the conditional distribution of model parameters given earthquake scenario is estimated by Monte Carlo simulation (MCS) using the regression model.

The regression model developed by Rezaeian and Der Kiureghian (2010) is

based on the data of far-field strong ground motions with magnitude larger than 6.0, which are able to yield structural damage as well as nonlinear behavior to structural system, so this regression model is used for BN model of main shocks. With the same stochastic model, Hu *et al*. (2018) developed regression models using of aftershocks. They present the regression models for two horizontal components of ground motions which are major and intermediate component. Among the regression models for two components, the model for major component is used for BN model of aftershocks. In Hu *et al*. (2018), the Joyner-Boore distance (R_{JB}) is additionally considered for the regression model of aftershock, which is the shortest distance between the site and the surface projection of the rupture surface (R_{rup} is the rupture distance which means the shortest distance between a site and a rupture surface). This approach requires more information about the fault to model the relationship between the Joyner-Boore distance and the rupture distance, so the Joyner-Boore distance is assumed to be the same as the rupture distance in this study. As a result, BN models for main shock and aftershocks are constructed using the same from of BN as shown in Figure 3.4, but the conditional distribution of model parameters are estimated using different regression models by Rezaeian and Der Kiureghian (2010) and Hu *et al*. (2018) respectively.

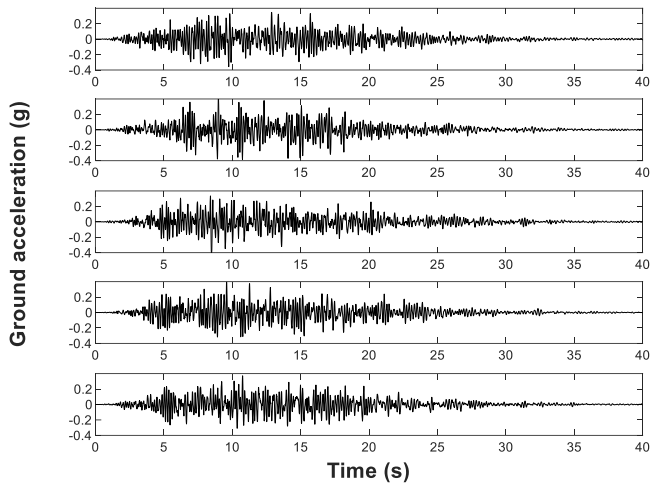

Figure 3.1 Simulated ground motions using $\bar{I}_{\mathrm{a}} = 0.244\mathrm{g}\cdot\mathrm{s}$, $D_{5-95} = 16.63\mathrm{s}$, $t_{mid} = 10.23\mathrm{s}$, $\omega_{mid}/2\pi = 5.71\mathrm{Hz}$, $\omega'/2\pi = -0.04\mathrm{Hz/s}$, $\zeta_f = 0.14$

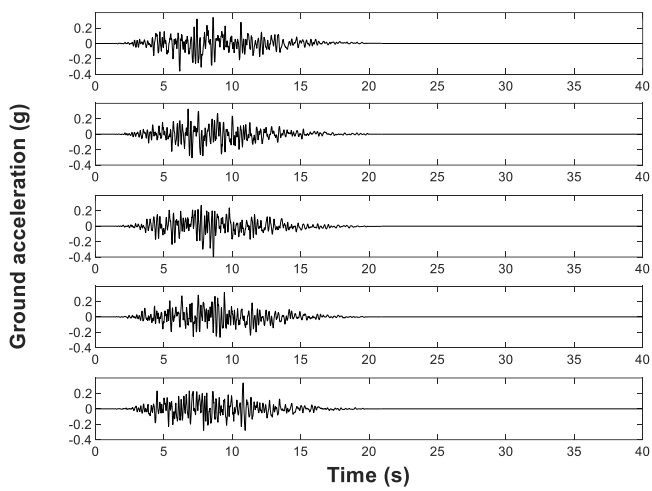

Figure 3.2 Simulated ground motions using $\bar{I}_{\mathrm{a}} = 0.109\mathrm{g}\cdot\mathrm{s}$, $D_{5-95} = 7.96\mathrm{s}$, $t_{mid} = 7.78\mathrm{s}$, $\omega_{mid}/2\pi = 4.66\mathrm{Hz}$, $\omega'/2\pi = -0.09\mathrm{Hz/s}$, $\zeta_f = 0.24$

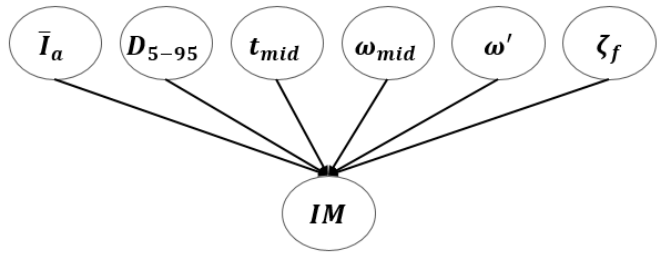

Figure 3.3 Bayesian network for the stochastic model

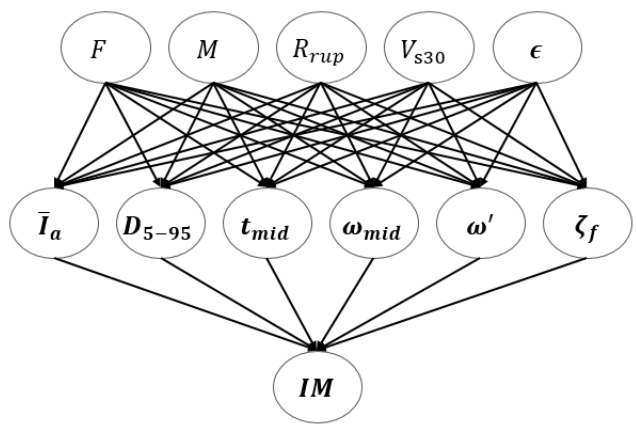

Figure 3.4 Bayesian network proposed for single ground motion

3.3. BN modeling of sequence of ground motions

As mentioned in Section 3.2., Hu *et al*. (2018) developed the regression model to estimate parameters of the stochastic model from a scenario of aftershock. In addition, they used a model to relate the scenario of aftershocks with the corresponding main shock to compare the simulated aftershocks with the real records of main and aftershocks. To this end, Hu *et al*. (2018) used the model termed the branching aftershock sequence (BASS; Turcotte *et al*. 2007). The BASS model randomly predicts the occurrence of aftershocks with its magnitude, location, and instance. This approach is used to relate BN models of main and aftershocks in this study. Especially, the largest magnitude among the predicted aftershocks with its relative distance is considered, which is estimated from the magnitude and rupture distance of main shock. The rupture type and site shear-wave velocity of aftershocks are assumed to be the same as the main shock as shown in Figure 3.5.

In the BASS model, an earthquake acts as a seed event, and triggers the following aftershocks. For example, a main shock triggers primary aftershocks, and the primary aftershocks trigger secondary aftershocks and so on. As the order of aftershocks increases, the number of occurrences and corresponding magnitudes gradually decrease. To focus on the risk right after the main shock, the seismicity of primary aftershocks, which are triggered by a main shock, are only considered in this study. The total number of aftershocks ($N_{d\mathrm{T}}$) induced by a seed main shock event is

$$N_{d\mathrm{T}} = 10^{b_d(m_p - \Delta m^* - m_{min})} \tag{3.9}$$

where m_p is the magnitude of a seed event; b_d, Δm^*, and m_{min} are parameters specified by regional properties. For each $N_{d\mathrm{T}}$ aftershocks, the magnitude (m_d) of

each aftershocks is randomly determined by solving the equation

$$P_{Cm} = 10^{-b_d(m_d - m_{min})} \tag{3.10}$$

where P_{Cm} is a random variable uniformly distributed between 0 and 1. The radial distance r_d of each aftershocks relative to the location of main shock is determined by solving the equation

$$P_{Cr} = \frac{1}{\left(1+r_d/d \cdot 10^{0.5m_p}\right)^{q-1}} \tag{3.11}$$

where P_{Cr} is a random variable uniformly distributed between 0 and 1, and d is a parameter. The direction of aftershock is uniformly determined between 0 and 2π. The BASS model also estimates the time of occurrence of each aftershocks (t_d) from

$$P_{Ct} = \frac{1}{\left(1+\frac{t_d}{\tau(p-1)N_{dT}}\right)^{p-1}} \tag{3.12}$$

where P_{Ct} is a random variable range from 0 to 1, and τ and p are parameters. Hu *et al*. (2018) used the time window by Gardner and Knopoff (1974) and the distance window of $L = 0.02 \cdot 10^{0.5m_p}$ (km) to include acceptable aftershocks scenarios. This study used the time and distance window. For example, the aftershocks farther than L or later than the time window are rejected until the total N_{dT} aftershock scenarios are generated. Among the N_{dT} aftershocks, the maximum magnitude with its relative distance is considered to take into account the worst scenario of aftershocks. As a result, the estimated magnitude of aftershocks increases as the magnitude of main shock grows as shown in Figure 3.6.

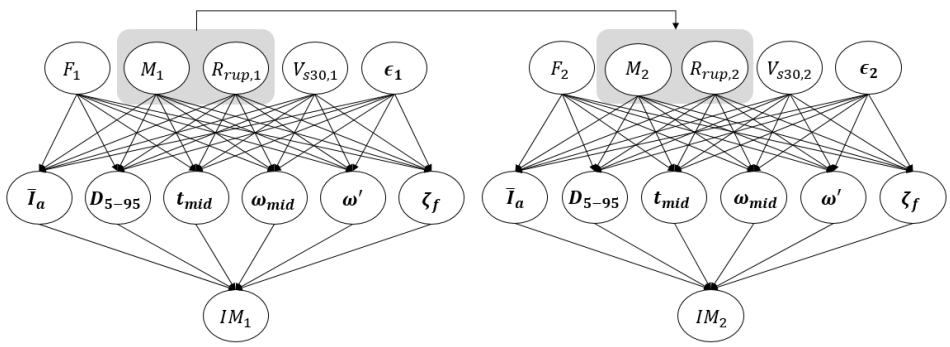

Figure 3.5 Bayesian network for sequence of main and aftershocks

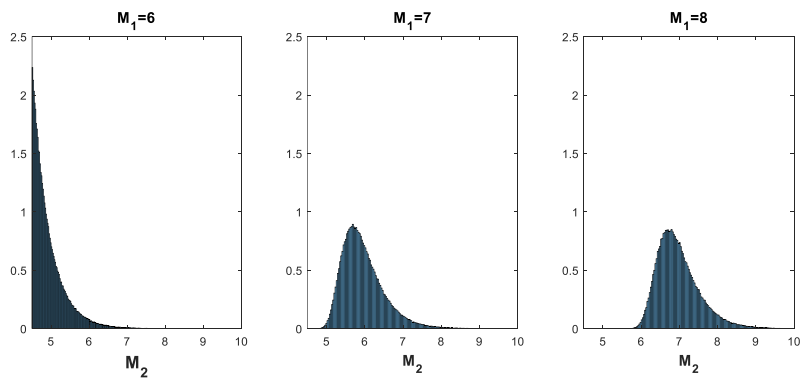

Figure 3.6 Histograms for estimated magnitude of aftershocks

Chapter 4. BN model of Structural System

4.1. Bouc-Wen class hysteresis

If structures are not damaged or degraded by main shock, additional risk assessment for possible aftershocks might not be a critical task because the fragility for aftershocks is usually less severe than main shock. However, if there exist some damage under main shock, the fragility for aftershocks will tend to increase, and upcoming aftershocks can be a fatal disaster. The damage can be considered as permanent deformation and deterioration of material property under the main shock. To reflect this in dynamic analysis, this study uses one of Bouc-Wen class models in which stiffness degradation can be modeled. The Bouc-Wen model is one of the most popular hysteresis models, which presented by Bouc (1967) and Wen (1976). Later, Baber and Noori (1985) modified the original Bouc-Wen model to facilitate describing degrading behavior, e.g. degradation of stiffness or strength, and pinching effect.

The Bouc-Wen class model is used to describe nonlinear relationship between displacement and resistance force. When a Bouc-Wen class model is used, the resistance force is divided into linear and nonlinear parts such as

$$f_s(x, \dot{x}, z) = \alpha k_0 x + (1 - \alpha) k_0 z \tag{4.1}$$

where x and $\dot{x}$ represent displacement and velocity respectively, k_0 is initial stiffness, α is the ratio of the post-yielding to initial stiffness, and z is auxiliary variable to explain nonlinear behavior. The auxiliary variable z is determined by

the displacement and velocity, which are described by the following differential equation (Barber and Noori 1985):

$$\dot{z} = \frac{A\dot{x} - \nu\{\beta|\dot{x}||z|^{n-1}z + \gamma\dot{x}|z|^{n}\}}{\eta} \tag{4.2}$$

where A, β, γ, and n are parameters related to the shape of hysteresis and ν and η are parameter related to the degradation of strength and stiffness respectively. The parameters A, ν, and η are defined as linear functions of hysteresis energy (ϵ), i.e.

$$\begin{aligned} A &= A_0 - \delta_A\epsilon \\ \nu &= 1 + \delta_\nu\epsilon \\ \eta &= 1 + \delta_\eta\epsilon \end{aligned} \tag{4.3}$$

in which the hysteresis energy is defined as time derivative $\dot{\epsilon} = (1-\alpha)k_0\dot{x}z$, and A_0, δ_A, δ_ν and δ_η are related parameters. Haukass (2004) presented the incremental form of the differential equation in Eq. 4.2 to facilitate implementation of the Bouc-Wen class model (so-called Bouc-Wen-Baber-Noori model) in computer codes. In this study, the stiffness degradation is only considered to reflect some damage from main shock, so δ_ν is assumed to be zero. Additionally, the parameter A is also set to one because it shows redundant performance on the model (Charalampakis and Koumousis 2010). For example, a typical relationship between resistance force and displacement of the Bouc-Wen-Baber-Noori model is shown in Figure 4.1.

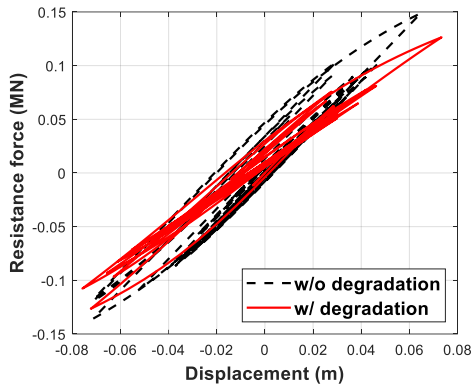

Figure 4.1 Typical Hysteresis of the Bouc-Wen-Baber-Noori model

4.2. BN modeling of structural system

The response of structural system is determined by the properties of system and ground motion. The characteristics of a dynamic system are usually explained by natural frequency (or natural period) and damping ratio. The seismic response of an ideal linear structure is defined by the properties, but nonlinear system requires additional information regarding its hysteresis behavior. In summary, natural frequency, damping ratio, and hysteresis can be used if the objective is to find the response for several type of structural systems.

The scope of this study is to construct a BN model for a single target structure, so the variation of response according to the properties of structures are not of interest. However, the state of the system can change due to earthquake event, and thus a variable to represent the state is needed. The damage under main shock is described by stiffness degradation of the Bouc-Wen-Baber-Noori model, which induces the change of the hysteresis property of the system as shown in Figure 4.1. To reflect the change (damage under main shock) in the BN model, the stiffness in elastic range after earthquake event is used, which is directly calculated from the incremental form of the Bouc-Wen-Baber-Noori model (Haukass 2004).

With the hysteresis model, dynamic analysis is performed sequentially with the generated ground motions of main and aftershocks. For example, for the sequence of generated ground motions in Figure 4.2, the response of a structural system (EDP) is calculated as shown in Figure 4.3. In the sequential analysis, residual deformation, which results from nonlinear behavior of structures, also affects the EDP of structures under aftershocks though it is not explicitly used as a random variable in the BN model. For an SDOF system, one variable representing EDP is needed to

define the failure of the system, e.g. peak displacement. The stiffness in elastic range of the system can be used to denote the varying state of the system under sequential earthquake events.

The EDPs calculated under main and aftershocks (EDP_1 and EDP_2), and the stiffness in elastic range before main shock (k_1), after main shock (k_2), and after aftershocks (k_3) can be represented in the BN model as shown in Figure 4.4. In Figure 4.4, the blue and green colored nodes denote the variables related to the main shock and aftershocks respectively. The red colored nodes denote the variables related to the structural system. Since the EDPs and damaged state (k_2 and k_3) result from the ground motions, they are connected with the ground motion model parameters. The EDP under aftershocks is also affected by the damaged state from main shock (k_2). In applications to real structures, the details on the relationship between random variables should be modified according to the type of structures. The conditional distributions of EDPs and the states of structure (k_2 and k_3) are estimated from the result of sequential dynamic analysis, and the accuracy of the conditional distribution will depend on the simulated ground motions which are based on the model parameters.

For a Multi Degree of Freedom (MDOF) system, multiple EDPs are needed to define the failure of the system. There are many EDPs used to define the failure such as maximum based shear, node rotations, the maximum inter-story drift ratio (IDR), or peak roof displacement (Vamvatsikos and Cornell 2002). In the proposed BN framework, any EDPs can be additionally added without modification of the proposed BN structure, which means that only the information of conditional distribution for the additional EDP is required. The stiffness of multiple DOFs can

be used to demonstrate the state of system (e.g. degradation). Other measures are also applicable to the BN model when different constitutive model is used to demonstrate the damage under main shock. In such consideration, the redundancy and cost of modeling should be taken into account to determine whether more features related to the damage of structures from main shock will be included. The structure of BN model for an MDOF system is described in Figure 4.5. The main structure can be used for various systems through modification according to the property of structure and constitutive models used in analysis.

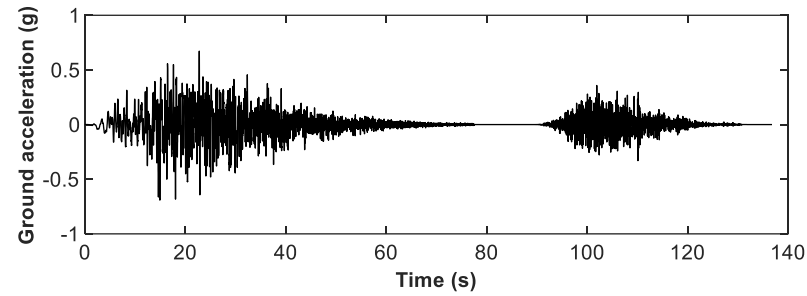

Figure 4.2 Example sequence of generated main and aftershock ground motions

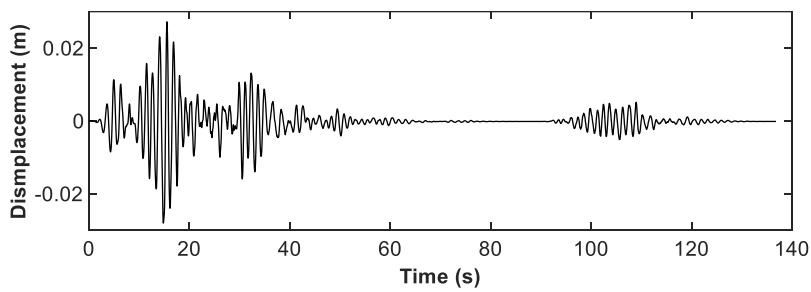

Figure 4.3 Response to the ground motion in Fig. 4.2

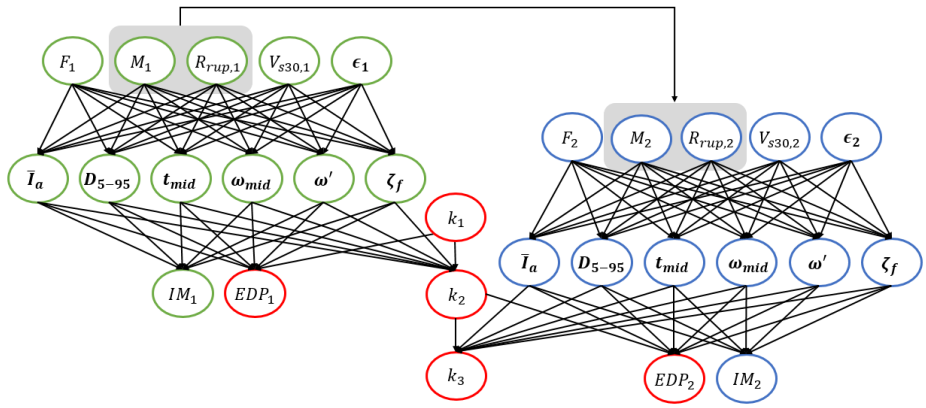

Figure 4.4 Bayesian network for an SDOF system under main and aftershocks

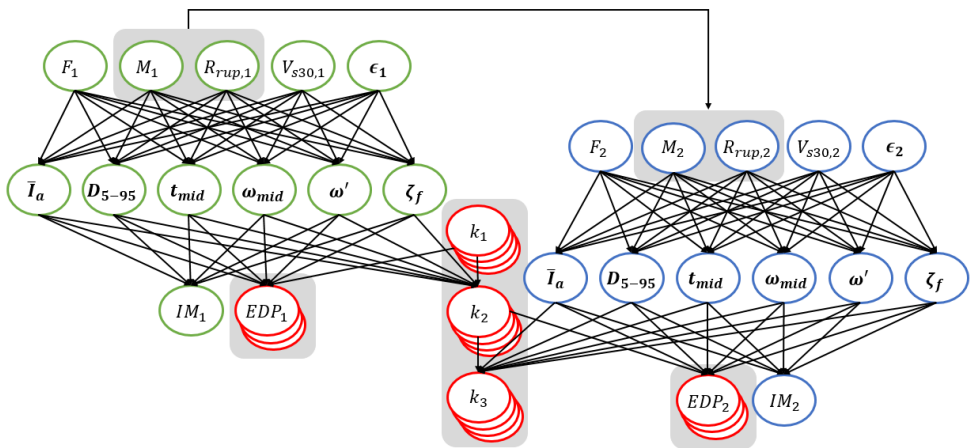

Figure 4.5 Bayesian network for an MDOF system under main and aftershocks

Chapter 5. Numerical Investigations

5.1. Ground motions used for BN modeling

The conditional distribution of each node is required to model the dependencies between random variables which are represented by nodes and arcs in BN graph. The conditional distributions of model parameters given earthquake scenario is directly estimated using the regression models for main and aftershocks described in Chapter 3. For example, samples of a specific scenario of main shock are transformed to the model parameters using the regression models (Rezaeian and Der Kiureghian 2010, Hu *et al*. 2018), and the conditional distribution is estimated from the transformed samples as illustrated in Figure 5.1 and 5.2.

IM is calculated from generated ground motions, and the corresponding EDP is computed by dynamic analysis of structural system. Accordingly, simulation strategy of main and aftershocks affects the estimated distribution of IM and EDP. In general BNs, the conditional distribution of child node is defined in the entire domain of parent nodes, i.e. exhaustive set, in the format of conditional probability table (CPT). For the CPT of IM and EDP, ground motions have to be simulated using the exhaustive set of the model parameters, which means that the model parameters need to be sampled in the hypercube in 6 dimension of which volume is

$$V = \prod_{i=1}^{6} (ub_i - lb_i) \tag{5.1}$$

where ub_i and lb_i for $i = 1, \dots, 6$ denote the upper and lower bounds of the model parameters, i.e. $\bar{I}_{\mathrm{a}}$, D_{5-95}, t_{mid}, ω_{mid}, ω', ζ_f. However, the joint

distribution of the model parameters are concentrated in the smaller subdomain of the volume V because they have correlation coefficient as well as they are not uniformly distributed within the boundaries. For example, Figure 5.3 shows the samples of D_{5-95} and t_{mid} from the joint distribution, which is distributed partially in rectangular area. Furthermore, the activated domain by the earthquake scenario is within the joint distribution of the model parameters, so the construction of CPT in the entire domain V is not needed. This also helps alleviate computer memory issue.

Matrix-based Bayesian network (MBN) was recently developed by Byun *et al*. (2019) to provide efficient modeling and inference in BN model. The MBN stores the information of conditional distribution in a matrix form, which is called conditional probability matrix (CPM). The CPM of child node is not necessarily required to be defined in exhaustive domain of parent nodes. In this study, the conditional distribution of EDP, IM, and the stiffness (k_2, k_3) are described by MBN, which enables sampling the model parameters having correlation. The correlation coefficients, which are given in Rezaeian and Der Kiureghian (2010) and Hu *et al*. (2018), are related to the inherent properties of ground motions. For example, the expected Arias intensity ($\bar{I}_{\mathrm{a}}$) have negative correlation with the 5-95% duration (D_{5-95}) since the ground motions with large amplitude tend to have short duration. By using the MBN, the child nodes of the model parameters are effectively modeled without simulation of unrealistic ground motions. In this study, 2,100 main shocks and 1,500 aftershocks are generated from the model parameters having correlation coefficients.

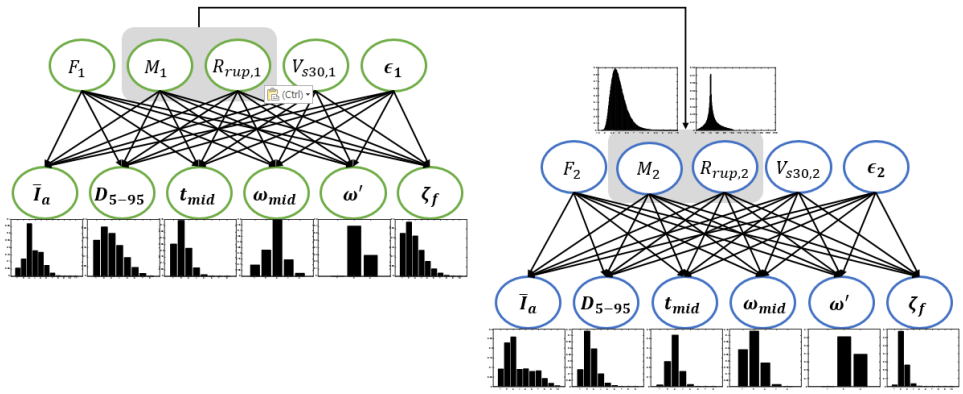

Figure 5.1 Conditional distribution of model parameters for main shock scenario ($M_1 = 7,\ R_{rup,1} = 40\text{km},\ F_1 = F_2 = \text{reverse},\ \text{V}_{s30,1} = 600\text{m/s}$)

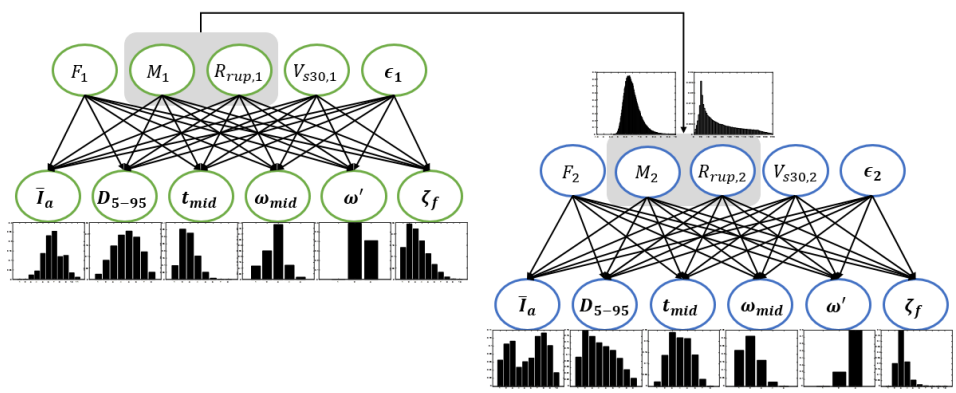

Figure 5.2 Conditional distribution of model parameters for main shock scenario ($M_1 = 8,\ R_{rup,1} = 20\text{km},\ F_1 = F_2 = \text{reverse},\ \text{V}_{s30,1} = 600\text{m/s}$)

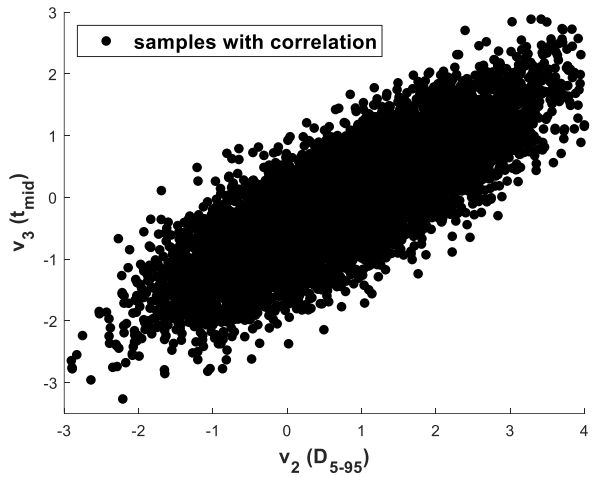

Figure 5.3 Joint distribution of D_{5-95} and t_{mid}

5.2. Fragility of an SDOF system

As described in Section 2.1, the fragility is the conditional failure probability of structural systems given the intensity of ground motion (IM). In a conventional approach, ground motions are selected to reflect the characteristics of the site where the system is located, so the fragility is actually depending not only IM but also the characteristics of site. This study selects the factors ($F,\ M,\ R_{rup},\ V_{\mathrm{s30}}$) to describe the site characteristics of ground motions, so the fragility is expressed as

$$\text{fragility} = \mathrm{P}(EDP \geq EDP_c | IM, F, M, R_{rup}, V_{s30}) \tag{5.2}$$

Eq. 5.2 corresponds to the posterior distribution of EDP given observation of IM and ($F,\ M,\ R_{\mathrm{rup}},\ V_{\mathrm{s30}}$). The fragility is calculated by using a BN inference. This study uses the inference algorithm of Matrix-based Bayesian Network (MBN) for which open source Matlab code by Byun *et al*. (2019) is available (https://github.com/jieunbyun/GitHub-MBN-code). In order to demonstrate the application of BN framework, an SDOF system with damping ratio 0.07, natural period 1.3s, and 2.5% noise in elastic range is investigated. The hysteresis behavior is described using the Bouc-Wen-Baber-Noori model with the parameters listed in Table 5.1. For the system, peak displacement and PGA are used as EDP and IM respectively.

In order to develop BN model of the SDOF system, the dependency of EDP and IM on the model parameters need to be checked. As mentioned in Section 3.1, the three model parameters ($\bar{I}_{\mathrm{a}},\ D_{5-95},\ t_{mid}$) are related to the parameters of the time modulating function ($\alpha_1,\ \alpha_2,\ \alpha_3$), which transform the shape of the normalized process. The other parameters ($\omega_{mid},\ \omega',\ \zeta_f$) have weak relationships with the

intensity of generated process because of the normalization after transformation of the white noise process. As a result, PGA depends only on the three model parameters ($\bar{I}_{\mathrm{a}},\ D_{5-95},\ t_{mid}$) which are related to the time modulating function. In contrast to the PGA, the peak displacement (D) is affected by both intensity and frequency contents of ground motions as shown in Figure 5.4.The conditional distribution of each node is defined to perform probabilistic inference. As explained in Section 5.1, the conditional distributions of model parameters are directly estimated by using the regression models presented in Rezaeian and Der Kiureghian (2010) and Hu *et al*. (2018). The conditional distribution of PGA and peak displacement (D) depend on the simulated ground motions, and 2,100 main shock and 1,500 aftershocks are used in this study. Using the ground motions, sequential dynamic analysis is performed, and the conditional distribution is calculated in the form of CPM. In the implementation of BN model, the model parameters are discretized with the boundaries presented in Table 5.2 and 5.3.

In the construction of CPM, using all model parameters as the parent nodes of PGA and peak displacement (D) would make the model excessively flexible to the given data, and thus the results of inference are unstable. This is because the generated ground motions do not cover the entire joint distribution of the model parameters, i.e. the used data are partially distributed in the domain of joint distribution. In order to relieve the flexibility, dependency on t_{mid} and ζ_f are not covered in this study. The final BN model of the SDOF system is presented in Figure 5.5. Using the BN model in Figure 5.5, the aftershock fragility is evaluated. In this evaluation, the aftershock fragility is conditioned not only the PGA of aftershocks but also that of the main shock. This enables us to take into account the structural

damage under the main shock. For the assumed scenario of main shock summarized in Table 5.4, the fragility is estimated as shown in Figure 5.6 and 5.7. The faults type and site shear-wave velocity of two scenarios are assumed to be the same, but the magnitude and rupture distance are assumed to introduce more dangerous earthquake in Case 2. For both cases, the aftershock fragility show larger failure probability as the PGA of main shock increases. This reflects the structural damage under main shock, in which more damage is expected for the main shock with higher PGA. The increment of aftershock fragility according to the PGA of main shock in Case 2 is larger than Case 1. This denotes that destructive ground motions are more likely to occur in Case 2, though the ground motion of main shock has the same PGA. The blue lines in Figure 5.6 and 5.7 are the frailty for main shock, and it is located inside the spectrum of aftershock fragility. This shows that the structures are more vulnerable to aftershocks when the structures are damaged to some extent.

The aftershock fragility is estimated according to the PGA of main shock. This subdivision enable us to find the fragility more specifically under sequential event. The PGA of main shock is indirectly used to represent structural damage, and the direct observation for the state of structural system can be made. The stiffness of the SDOF system is shown in Figure 5.8, in which the blue and orange histogram denote the stiffness before and after main shock respectively. For the aftershock fragility for $0.3 < PGA_1 < 0.4$ in Case 2, Figure 5.9 shows the aftershock fragility which is updated with the information about stiffness. The observed (assumed) information is whether the stiffness after main shock (k_2) is larger or smaller than a prescribed value $k_0 = 2.1\text{MN/m}$ in Figure 5.8. The result in Figure 5.9 shows that the more information enable us to estimate more accurate fragility for the specific condition.

Table 5.1 Parameters of the Bouc-Wen-Baber-Noori model

Parameter	Value
α	0.01
A	1
n	1.78
γ	36.34
β	36.34
δ_v	0
δ_η	0.00002

Table 5.2 Discretization of model parameters for main shock

Main shock	
$\bar{I}_{\mathrm{a}}$ (g·s)	[0, 0.005, 0.01, 0.03, 0.05, 0.1, 0.2, 0.4, 0.6, 1.2, 1.8, 2.34]
D_{5-95} (s)	[5, 10, 15, 20, 25, 30, 40, 45]
t_{mid} (s)	[0.5, 5, 10, 15, 20, 25, 30, 35, 40]
$\omega_{mid}/2\pi$ (Hz)	[1, 3, 5, 10, 15, 21.6]
$\omega'/2\pi$ (Hz/s)	[-2, -0.2, 0, 0.5]
ζ_f	[0.02, 0.1, 0.2, 0.3, 0.4, 0.5, 0.6, 0.7, 0.8, 0.9, 1]

Table 5.3 Discretization of model parameters for aftershocks

Aftershock	
$\bar{I}_{\mathrm{a}}$ (g·s)	[0, 0.0005, 0.0015, 0.004, 0.006, 0.01, 0.018, 0.05, 0.15, 0.4, 0.6]
D_{5-95} (s)	[5, 10, 15, 20, 25, 30, 40, 45]
t_{mid} (s)	[0.5, 5, 10, 15, 20, 25, 30, 35, 40]
$\omega_{mid}/2\pi$ (Hz)	[1, 3, 5, 10, 15, 21.6]
$\omega'/2\pi$ (Hz/s)	[-2, -0.2, 0, 0.5]
ζ_f	[0.02, 0.1, 0.2, 0.3, 0.4, 0.5, 0.6, 0.7, 0.8, 0.9, 1]

Table 5.4 Earthquake scenarios of main shock

	Case 1	Case 2
F	reverse	reverse
M	7	8
R_{rup} (km)	40	20
V_{s30} (m/s)	600	600

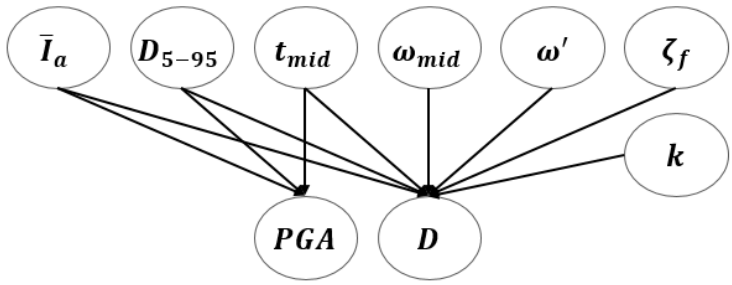

Figure 5.4 Dependency of PGA and peak displacement (D) on the model parameters described in BN model

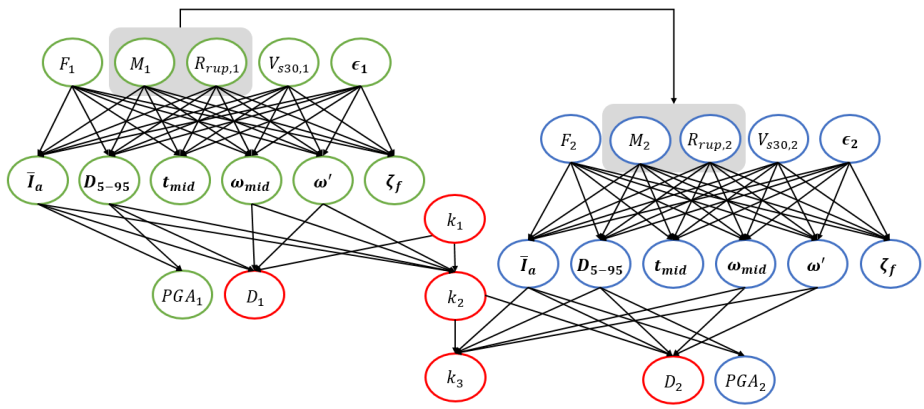

Figure 5.5 Bayesian network of an SDOF system used for fragility assessment

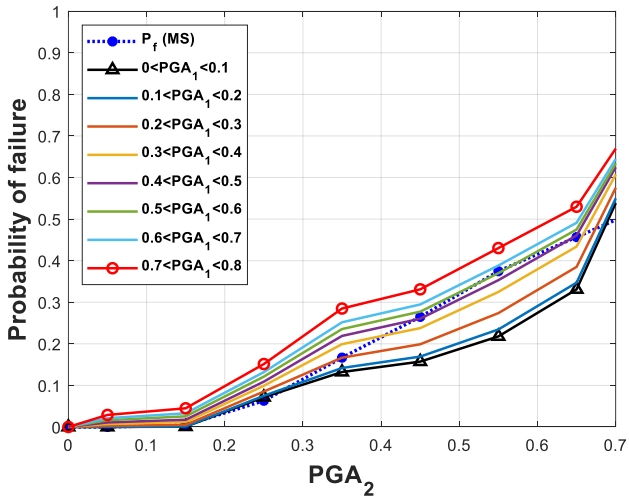

Figure 5.6 Fragility of the SODF system for aftershocks in Case 1

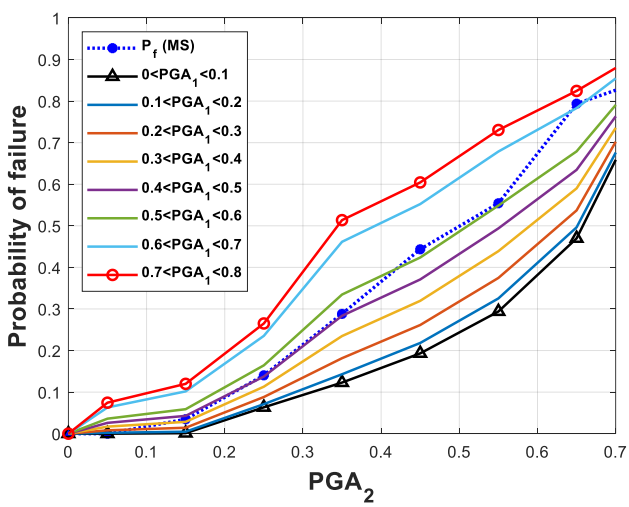

Figure 5.7 Fragility of the SDOF system for aftershocks in Case 2

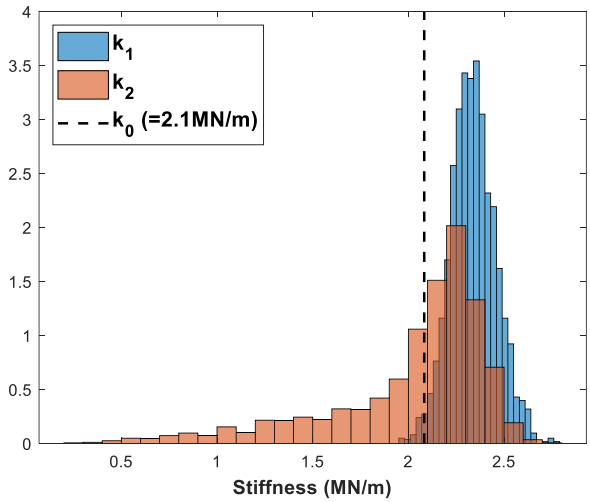

Figure 5.8 Histograms of stiffness before main shock (blue) and after main shock (orange)

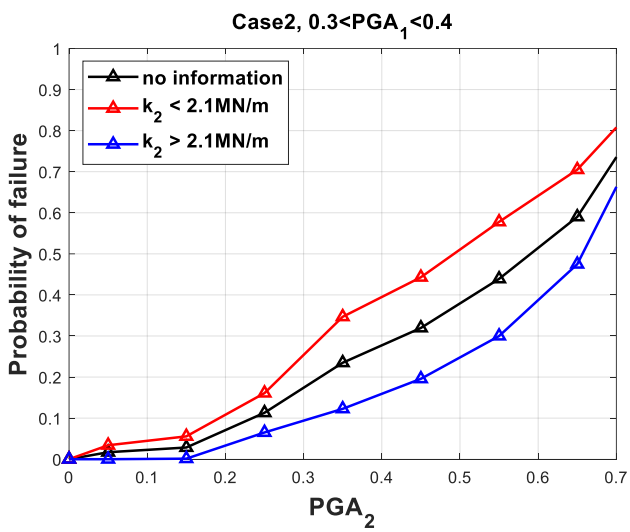

Figure 5.9 Fragility updated by the information about stiffness

5.3. Fragility of an MDOF system

For general application of the BN framework, 5-DOF shear building model in Figure 5.10 is considered. All the stories except the first story are modeled linearly with stiffness $k = 100{,}000\text{kN/m}$ but the first story is modeled by the Bouc-Wen-Baber-Noori model with initial stiffness $k_0 = 100{,}000\text{kN/m}$. Each story has the same mass $m = 40{,}000\text{kg}$ and height $h = 3.5\text{m}$. For the first and third modes in elastic range, 7% of Rayleigh damping is assumed.

Maximum inter-story drift ratio (IDR) and peak roof displacement (RD) are used as EDPs, while the stiffness of the first floor is used as the variable representing the change of state from the damage under earthquake event. The BN for the 5-DOF shear building is represented in Figure 5.10. Using the BN model of 5-DOF system, aftershock fragility for each EDP (IDR, RD) can be estimated. For the uniformly assumed scenarios (Table 5.5), the aftershock fragilities for each EDPs are estimated using the BN model as shown in Figure 5.11 and 5.12. The failure events by IDR and RD are not exclusive to each other, so a series event of IDR and RD is also considered, that is, the fragility is defined as

$$\mathrm{P}((IDR > IDR_c) \cup (RD > RD_c) | PGA_2) \tag{5.3}$$

where $\cup$ is the set operator of union event. Figure 5.13 shows the fragility for the union event. This example shows that the BN model can be extended to multiple EDPs of interest. The fragility for the union event with the multiple EDPs is then estimated by the BN model without constructing a new seismic sequence model.

Table 5.5 Earthquake scenario for main and aftershocks

	Main shock	Aftershocks
F	Reverse, Strike-slip	Reverse, Strike-slip,
M	[6, 8]	[4.5, 7]
R_{rup} (km)	[10, 100]	[10, 80]
V_{s30} (m/s)	[600, 900]	[250, 900]

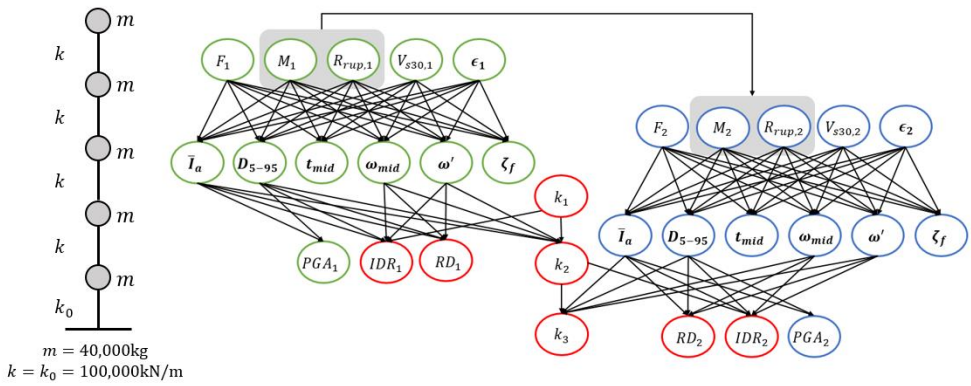

Figure 5.10 5-DOF shear building model (left) and corresponding BN model (right)

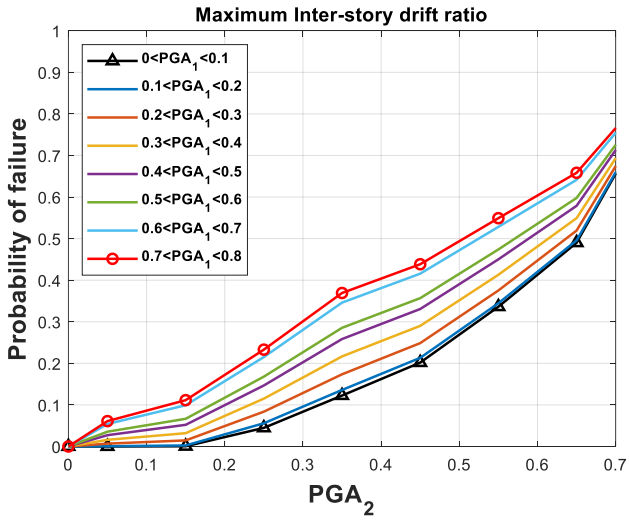

Figure 5.11 Fragility of the 5-DOF system for aftershocks (EDP: IDR)

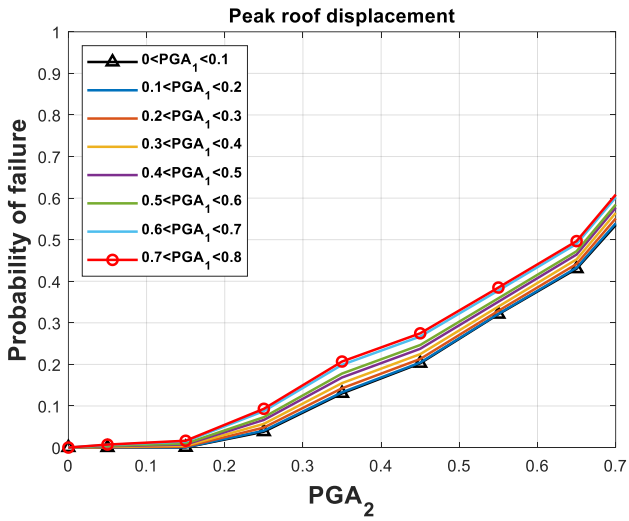

Figure 5.12 Fragility of the 5-DOF system for aftershocks (EDP: RD)

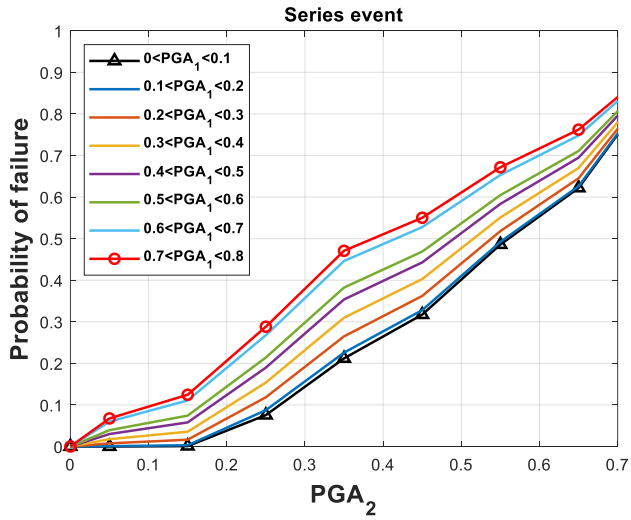

Figure 5.13 Fragility of the 5-DOF system for aftershocks (EDPs: IDR and RD)

Chapter 6. Conclusion

In this study, a Bayesian network (BN) model of the sequence of main and aftershocks is developed for the purpose of fragility assessment of structural systems. Earthquake scenarios of main and aftershocks are modeled by BN for comprehensive description its correlation, characteristics of ground motions, and structural response with structural damage under sequential earthquake. The relationship between the features are displayed intuitively in the graphical structure of the BN model. The developed BN model presents a new framework to evaluate the fragility of structures, and facilitates updating aftershock fragility using the information related to the aftermath of main shock. In order to construct the BN model, ground motions are simulated using the stochastic model whose parameters constitute the BN model to relate the intensity of ground motions (IM) with structural response (EDP). This representation enables us to encompass consistent domain of ground motion regardless of the type of IM. In the proposed process, the Matrix-based Bayesian network (MBN) is used for efficient modeling of the BN structure. The numerical examples of SDOF and MDOF systems are investigated to show the applicability and capability of the BN framework. It is also shown that multiple IMs and EDPs can be incorporated without changing the ground motion set.

Though the BN model is applicable to general structural systems, the study related to the construction of BN model has not been considered elaborately for wider class of problems. The sampling of model parameters and discretization of random variables should be also further investigated to ensure a desirable level of accuracy. Further development of each of the model, which constitute the BN model (e.g. regression models), would enhance the performance of the proposed BN methodology. This improvement will provide more accurate evaluation of fragility and insight about aftershocks and their impact.

Reference

A. E. Charalampakis and V. K. Koumousis, “Parameters of Bouc-Wen model revisited”, *9th HSTAM Internation Congress on Mechanics,* 2010

A. Miano, F. Jalayer, H. Ebrahimian, and A. Prota, “Cloud to IDA: Efficient fragility assessment with limited scaling”, *Earthquake Engineering and Structural Dynamics*, 2018, Vol. 47, pp. 1124-1147

C. Zhai, W. Wen, S. Li, Z. Chen, Z. Chang, and L. Xie, “The damage investigation of inelastic SODF structure under the mainshock-aftershock sequence-type ground motions”, *Soil Dynamics and Earthquake Engineering,* 2014, Vol. 59, pp. 30-41

D. Vamvatsikos and C. A. Cornell, “Incremental dynamic analysis”, *Earthquake Engng Struct. Dyn*. 2002, Vol. 31, pp. 491-514

D. L. Turcotte, J. R. Holliday, and J. B. Rundle, “BASS, an alternative to ETAS”, *Geophysical Research Letters,* 2007, Vol. 34

D. Koller and N. Friedman, “Probabilistic graphical models: principles and techniques”, *Cambridge: The MIT Press,* 2009

F. Jalayer, “Direct probabilistic seismic analysis: Implementing non-linear dynamic assessments”, *Ph.D. dissertation,* 2003

F. Jalayer, R. D. Risi, and G. Manfredi, “Bayesian Cloud Analysis: efficient structural fragility assessment using linear regression”, *Bulletin of Earthquake Engineering*, 2015, Vol. 13, pp. 1183-1203

H. Ryu, N. Luco, S. R. Uma, and A. B. Liel, “Developing fragilities for mainshock-

damaged structures through incremental dynamic analysis", *9th Pacific Conference on Earthquake Engineering*, 2011

I. Iervolino, G. Manfredi, and E. Cosenza, "Ground motion duration effects on nonlinear seismic response", Earthquake Engineering and Structural Dynamics, 2006, Vol. 35, pp. 21-38

J. K. Gardner and L. Knopoff, "Is the sequence of earthquakes in southern California with aftershocks removed, poissonian?", *Bulletin of the Seismological Society of America*, 1974, Vol. 64, pp. 1363-1367

J. Moehle and G. G. Delerlein, "A framework methodology for performance-based earthquake engineering", *13 WCEE*, 2004

J. Shin, J. Kim, and K. Lee, "Seismic assessment of damaged piloti-type RC building subjected to successive earthquakes", *Earthquake Engineering and Structural Dynamics*, 2014, Vol. 43, pp. 1603-1619

J. W. Baker (2015), "Efficient analytical fragility function fitting using Dynamic structural analysis", *Earthquake Spectra*, 2015, Vol 31, pp. 579-599

J. Byun, K. Zwirglmaier, D. Straub, and J. Song, "Matrix-based Bayesian Network for efficient memory storage and flexible inference", *Reliability Engineering and System Safety*, 2019, Vol. 185, pp. 533-545

M. Shinozuka and G. Deodatis, "Simulation of stochastic processes by spectral representation", *Applied Mechanics Reviews*, 2009, Vol. 44(4), pp. 191-204

R. Bouc, "Forced vibration of a mechanical system with hysteresis", *4th Conference on Non-linear Oscillations*, 1967

S. Rezaeian and A. D. Kiureghian, "A stochastic ground motion model with

separable temporal and spectral nonstationarities", *Earthquake Engineering and Structural Dynamics*, 2008, Vol. 37, pp. 1565-1584

S. Rezaeian and A. D. Kiureghian, "Simulation of synthetic ground motions for specified earthquake and site characteristics", 2010, Vol. 39, pp. 1155-1180

T. Baber, and M. Noori, "Random vibration of degrading pinching systems", *Journal of Engineering Mechanics*, 1985, Vol. 111(8), pp.

T. Haukaas, "Finite Element Reliability and Sensitivity Methods for Performance-Based Engineering", *Ph.D. dissertation*, 2003

Y. Wen, "Method for random vibration of hysteretic systems", *Journal of the Engineering Mechanics Division*, 1976, Vol. 102(2), pp. 249-263

국문 초록

지진 등 큰 피해를 일으키는 자연재해에 대한 안전한 사회 인프라를 구축하기 위해 재해가 유발하는 다양한 리스크를 종합적으로 평가하여야 한다. 강한 지진이 발생할 경우 수차례의 여진을 동반하는데, 본진에 의한 구조물 손상 정도에 따라 여진에 대한 피해는 크게 증가한다. 따라서 본진과 여진을 복합적으로 고려하여 향후 발생할 여진에 대한 리스크 평가가 진행되어야 한다. 이를 위해 위해 본진-여진 시퀀스가 가지는 불확실한 특성들과, 본진에 의해 생기는 구조물 손상을 고려할 수 있는 확률모델이 필요하다.

이러한 본진-여진 사건에 대한 확률모델을 구축하기 위해 베이지안 네트워크가(Bayesian Network) 사용되었다. 베이지안 네트워크는 많은 변수들에 대한 확률모델을 효과적으로 구축할 수 있는 방법론이다. 또한 베이지안 네트워크 모델을 이용한 확률추론을 통해, 계측된 정보로부터 변수들의 상태를 업데이트 할 수 있는 장점이 있다. 베이지안 네트워크에서 확률변수와 이들의 관계는 노드 및 화살표로 표현되며, 변수들의 관계에 상응하는 조건부 확률분포를 통해 확률모델이 정의된다.

본 연구에서는 본진-여진에 대한 특성들을 반영하기 위해 인공지진가속도를 사용하였다. 또한 구조물의 손상을 묘사할 수 있는 구조모델을 사용하여 생성된 본진과 여진 인공 지진가속도에 대해

연속적으로 구조해석을 수행하였다. 이 과정에서 발생하는 중요한 정보들을 확률변수로 선정하였으며, 본진-여진 복합재해에 대한 종합적인 평가가 가능한 베이지안 네트워크를 구축하였다. 이때, 기존의 베이지안 네트워크에서 취약도 평가에 불필요한 정보도 조건부 확률분포로 구축해야 하는 비효율성을 해결하기 위해 최근 제안된 행렬기반 베이지안 네트워크(Matrix-based Bayesian Network)를 사용하여 효율적으로 확률모델을 구축하였다.

최종적으로 구축된 베이지안 네트워크를 이용하여 본진-여진 사건에서 여진에 대한 구조물의 취약도(Fragility)를 평가하였다. 취약도는 특정 강도를 지니는 지진이 왔을 때 구조물이 파괴될 확률로 베이지안 네트워크의 확률추론 기능을 이용해 평가할 수 있다. 본 연구에서는 베이지안 네트워크를 통해 본진과 여진의 특성을 함께 고려한 취약도 평가를 하였으며, 이를 통해 구조물의 손상이 클수록 향후 다가올 여진에 대해 취약도가 증가하는 것을 정량적으로 나타내었다. 이러한 베이지안 네트워크를 이용한 본진-여진 사건에 대한 확률모델 구축 및 취약도 평가는 수치예제를 통해 제시되었다.

주요어: 본진, 여진, 베이지안 네트워크, 행렬기반 베이지안 네트워크, 확률추론, 취약도

학번: 2017-28720